

Disordered state resulting from spin flip in $Y_{0.1}Lu_{0.9}CrO_3$ induced by an external magnetic field with competing anisotropy

V. N. Milov, G. G. Artem'ev, V. I. Nedel'ko, A. F. Prun, M. V. Semenova, and E. V. Sinitsyn

M. V. Lomonosov State University, Moscow

(Submitted 4 July 1984)

Zh. Eksp. Teor. Fiz. **88**, 272–279 (January 1985)

The monoclinic magnetostriction and torque in $Y_{0.1}Lu_{0.9}CrO_3$ were measured at $T = 4.2$ K in fields ≤ 40 kOe in order to investigate partial disordering of the $G(F)$ spin system during the $\Gamma_2 \rightarrow \Gamma_4$ spin-flip transition in compounds with competing anisotropy. The experimental studies indicate that external-magnetic-field-induced spin-flip transitions from the Γ_2 phase in $Y_{0.1}Lu_{0.9}CrO_3$ give rise to a magnetic structure in which the dispersion $D(\theta)$ of the orientation fluctuations and the average magnetic moment $F(\theta)$ are orientation-dependent. This dependence is typical for systems with competing magnetic anisotropy and causes characteristic anomalies in the torques and magnetostriction.

Diverse random magnetic structures are found in systems with competing anisotropic interactions,¹ and studies of such systems are of great interest in the investigation of novel types of magnetic ordering. Disordered solid solutions based on rare-earth perovskites ($RFeO_3$, $RCrO_3$) are convenient materials for study, because the microscopic mechanisms which determine the magnitude and sign of the magnetic anisotropy constants have been studied quite well for these compounds, so that systems with a controllable competitive anisotropy can be synthesized. For example, the magnitude and sign of the magnetic anisotropy constant for the chromium atom in the compounds $Y_xLu_{1-x}CrO_3$ are sensitive to the degree of distortion of the $Cr^{3+}-6O^{2-}$ octahedra (Ref. 2), which in turn is determined by the ionic radii of the rare-earth elements. In particular, the anisotropy constant is positive for $YCrO_3$ and the compound exists in the phase $\Gamma_4(G_x F_x)$ (where F and G are the ferro- and antiferromagnetic vectors of the orthochromites, respectively); by contrast, the anisotropy is negative in $LuCrO_3$, where the $\Gamma_2(G_z F_x)$ phase occurs.² Because of the random distribution of the Y and Lu ions over the lattice sites in the mixed orthochromites $Y_xLu_{1-x}CrO_3$, the local anisotropy fields acting on the Cr ions differ in magnitude and sign. If the average magnetic anisotropy constant is positive and exceeds a critical value, the Γ_4 phase occurs, while if this constant is less than a certain negative value, the Γ_2 phase is stable.³

The $G(F)$ vectors are collinear and in equilibrium away from the spin-flip transition. Near this transition (produced,

e.g., by an external magnetic field), the $G(F)$ vectors (which are coupled by exchange processes) are acted upon by the torques produced by the local magnetic anisotropy, which tend to deflect each of the vectors $G(r)$, $F(r)$ toward the local easy axis at the point r . This makes the distribution of F , G spatially nonuniform and causes a dispersion in the angles $\theta(r)$ which specify the orientation of $G(r)$, $F(r)$ relative to the crystallographic axes. Since the magnetic anisotropy energy in $Y_{0.1}Lu_{0.9}CrO_3$ is much less than the exchange energy, the angle between two adjacent vectors $G(F)$ must be very small. However, it was shown in Ref. 3 that the dispersion $D(\bar{\theta})$ in the orientation of the antiferromagnetic vector may be substantial over the entire volume of the crystal, and $D(\bar{\theta}) \sim \sin^2(2\bar{\theta})$ (here $\bar{\theta} = \langle \theta(r) \rangle$ is the angle between the easy magnetization axis of the system and the vector $\langle G \rangle$ averaged over the crystal).

The above arguments imply that the spin system may become partly disordered and the average magnitudes of G and F in the angular phase Γ_{24} may decrease during a spin-flip transition in systems with competing anisotropy (Fig. 1.).

SAMPLES AND MEASUREMENT METHOD

The vectors G and F are known to respectively determine the magnetoelastic deformations and torque in perovskites. We therefore measured the longitudinal and transverse magnetostrictions, the monoclinic distortions, and the torque for several crystal planes at $T = 4.2$ K. The field de-

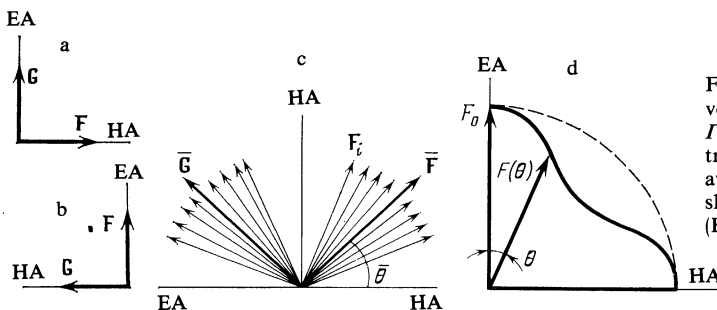


FIG. 1. Model for the spin system in $Y_{0.1}Lu_{0.9}CrO_3$: a) position of the vectors G and F in the $\Gamma_4(G_x F_x)$ phase; b) the vectors G and F in the $\Gamma_2(G_z F_x)$ phase; c) onset of partial ordering of G and F during the spin-flip transition in the Γ_{24} angular phase; d) decrease in the magnitude of the average vector $\langle F \rangle$ during the spin-flip transition. The dashed curve shows how F changes during a spin-flip transition with partial ordering (EA and HA denote the easy and hard axes of magnetization).

pendences were measured in pulsed magnetic fields ≤ 50 kOe by means of a piezoelectric quartz sensor bonded directly to the sample. The relative measurement error was less than 3%. We also used a self-compensating torque magnetometer to record the angular dependences of the torque in static fields between 2 and 15 kOe.

M. M. Lukina grew the LuCrO_3 and $\text{Y}_{0.1}\text{Lu}_{0.9}\text{CrO}_3$ crystals from solution in a melt containing lead compounds.

EXPERIMENTAL RESULTS

The longitudinal and transverse magnetostrictions were measured in the ac -plane of a $\text{Y}_{0.1}\text{Lu}_{0.9}\text{CrO}_3$ single crystal in Ref. 4, where the spin subsystem of the chromium ions was found to become ordered into the Γ_4 phase for T below the Néel temperature $T_N = 112$ K. A spontaneous spin-flip transition to the Γ_2 phase occurs as T drops in the interval 95–80 K, and this phase remains stable down to 4.2 K. It was shown in Ref. 5 that the reduced magnetic symmetry in the angular Γ_{24} phase during $\Gamma_2 \rightarrow \Gamma_4$ spin-flip process reduces the crystal symmetry of the orthochromite from rhombic to monoclinic, i.e., the angle between the crystallographic axes changes. This results in a shearing deformation (called monoclinic distortions below) which is related to the position of the vector \mathbf{G} by

$$\lambda_{ac} = \lambda_{ac}^{(0)} G^2 \sin 2\theta, \quad (1)$$

where $\lambda_{ac}^{(0)}$ is the magnetoelastic constant.

We will take θ and G in (1) to be given by $\bar{\theta}$ and $|\langle \mathbf{G} \rangle|$, respectively, for disordered materials with a spatially non-uniform distribution $\mathbf{G}(\mathbf{r})$.

Figure 2a shows the field dependences of the monoclinic magnetostriction for $\text{Y}_{0.1}\text{Lu}_{0.9}\text{CrO}_3$ at $T = 4.2$ K for several orientations φ of the magnetic field relative to the easy axis in the ac -plane. Since a change in the orientation of the applied field from $+\varphi$ to $-\varphi$ reversed the sign of the magnetostriction while leaving its magnitude unchanged, the magnetostriction may be attributed to purely monoclinic distortions of the crystal. The curve with $\varphi = 90^\circ$ was recorded by applying the field at an angle of 0.5° to the c -axis in

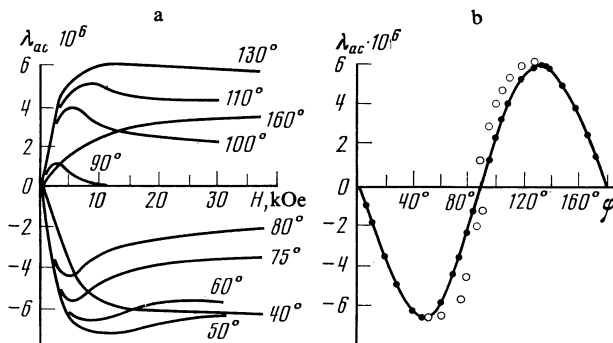


FIG. 2. a: Field dependences of the monoclinic magnetostriction λ_{ac} in $\text{Y}_{0.1}\text{Lu}_{0.9}\text{CrO}_3$ at $T = 4.2$ K for several magnetic field orientations (indicated alongside the curves) relative to the easy a -axis in the ac -plane. b: Angular dependence of λ_{ac} in a field $H = 28$ kOe (dark circles on the sine curve) and maximum magnetostrictions λ_{ac}^{\max} (open circles) in $\text{Y}_{0.1}\text{Lu}_{0.9}\text{CrO}_3$ for several applied field angles.

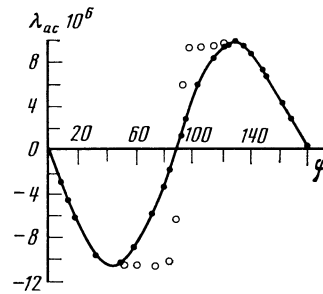


FIG. 3. Dependence $\lambda_{ac}(\varphi)$ at saturation in a field $H = 12$ kOe (dark circles on the sine curve) and the maximum magnetostrictions λ_{ac}^{\max} for several applied field angles (open circles) in LuCrO_3 at $T = 4.2$ K.

order to study the single-domain initial state. As the applied field H increases, $\bar{\theta}$ varies from 0 to $\bar{\theta} \approx \varphi$. Figure 2a and Eq. (1) show that the dependence $\bar{\theta}(H)$ is smooth (there are no jumps). The monoclinic deformation changes in accordance with Eq. (1): it increases to a maximum for $\bar{\theta} = 45^\circ$ and then falls off, tending to the value $\lambda_{ac}^{(0)} G^2 \sin(2\varphi)$ for above-threshold field strengths.

However, $\text{Y}_{0.1}\text{Lu}_{0.9}\text{CrO}_3$ differs significantly in several respects from the compound YCrO_3 studied in Ref. 6, as well as from LuCrO_3 , whose monoclinic magnetostriction at saturation is shown in Fig. 3 as a function of φ for $H = 12$ kOe, along with the maximum magnetostrictions λ_{ac}^{\max} for different φ . For LuCrO_3 the peak values $\lambda_{ac}^{\max}(H)$ are the same for all φ between 45° and 90° , in agreement with Eq. (1). Indeed, the peaks λ_{ac}^{\max} are all reached when \mathbf{G} passes through the orientation $\bar{\theta} = 45^\circ$ in the ac -plane, which is the reason why the deformations $\lambda_{ac}^{(0)} G^2$ are all the same, $G^2 = \text{const}(\varphi)$.

Figure 2a, b shows curves $\lambda_{ac}(\varphi)$ in a field $H = 28$ kOe which are analogous to the ones for LuCrO_3 ; here however we see that the peak values λ_{ac}^{\max} are different for $45^\circ < \varphi < 90^\circ$. The maxima are largest, $\lambda_{ac}^{\max} = 6.5 \cdot 10^{-6}$, for the field angle $\varphi = 45^\circ$. For fields almost parallel to the hard axis ($\varphi = 88^\circ$), $\lambda_{ac}^{\max} = 1.2 \cdot 10^{-6}$, i.e., is slightly more than 20% of the value for $\varphi = 45^\circ$. For fields above threshold, the angular dependence $\lambda_{ac}(\varphi)$ for $\text{Y}_{0.1}\text{Lu}_{0.9}\text{CrO}_3$ is closely described by the theoretical sinusoidal dependence (1).

Measurements of the monoclinic distortions in the ab - and bc -planes revealed that the vector \mathbf{G} rotates in the ac -plane. The domain structure had no influence on λ_{ac}^{\max} for φ in the range investigated because the demagnetization occurred for much weaker fields $H \sim 100$ Oe. We may thus conclude that $\mathbf{G} = |\mathbf{G}|$ depends on θ during the $\Gamma_2 \rightarrow \Gamma_4$ spin-flip transition: in the Γ_{24} angular phase, G is less than G_0 in Γ_2 and Γ_4 and reaches the maximum value of G_0 only in very strong fields. This behavior is consistent with a degree of disordering of the vectors \mathbf{G} in the crystal.

The dependence of G on the orientation of \mathbf{G} suggests a similar dependence for the weak ferromagnetic moment \mathbf{F} . We can observe this dependence by measuring the torque in the ac -plane. Figure 4 shows the field dependences of the torque in $\text{Y}_{0.1}\text{Lu}_{0.9}\text{CrO}_3$ for $T = 4.2$ K and several field orientations in the ac -plane. The torque vanishes for H nearly parallel to the a -axis of the crystal, i.e., \mathbf{F} points along the a -axis and the spins are in the Γ_2 configuration. For fields

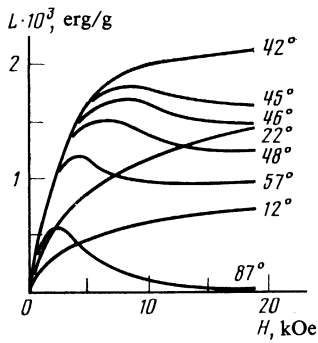


FIG. 4. Field dependences of the torque in $Y_{0.1}Lu_{0.9}CrO_3$ at $T = 4.2$ K for several field orientations in the ac -plane (indicated alongside the curves).

along the c -axis, the angular dependence of the torque is bell-shaped with a peak of $L^{\max} = 250$ erg/g, i.e., the field initiates the Γ_4 phase and $\theta = \varphi$ if $H \gg H_{\text{thr}}$. For fields making a 45° angle with the a -axis, L exceeds $2 \cdot 10^3$ erg/g at saturation. It is clear from Fig. 4 that L^{\max} differs along the isotherms for different φ .

The form of the curves $\lambda_a(H)$ in Fig. 5a implies that the dependence $\theta(H)$ is continuous and monotonic increasing. As it rotates in the field, the weak ferromagnetic moment passes sequentially through all states from $\theta = 0$ to $\theta \approx \varphi$ for fields $H > H_{\text{thr}}$. If moreover we assume that $G = \text{const}$ and $F = \text{const}$, $L(H)$ must take on all values from 0 to $L(\theta)|_{\theta \approx \varphi}$, including the value $L^{\max}(H)$, which is the same for all $\varphi > 45^\circ$. Although this approach correctly describes the $L(H)$ dependence for $YFeO_3$ (Ref. 7) and $YCrO_3$, it cannot account for the behavior of the $L(H)$ isotherms for $Y_{0.1}Lu_{0.9}CrO_3$ (Fig. 4).

Figure 6a shows the angular dependence $L(\varphi)$ for $H = \text{const}$ (8 kOe, 15 kOe) deduced from the above $L(H)$ field dependences; the curve $L(\varphi)$ is equivalent to the one found by rotating a constant magnetic field in the ac -plane of the crystal. We see that $L(\varphi)$ drops sharply for $\varphi \sim 45^\circ$, and the magnitude of the drop for $H = 15$ kOe is almost twice the magnitude for $H = 8$ kOe.

Although these $L(\varphi)$ angular dependences are unusual for orthochromites, they can also be explained in terms of

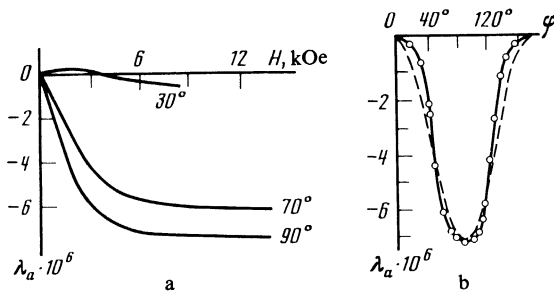


FIG. 5. Field (a) and angular dependences (b) of the quadratic magnetostriiction λ_a in $Y_{0.1}Lu_{0.9}CrO_3$ at $T = 4.2$ K for several orientations φ of the magnetic field relative to the a -axis (indicated alongside the curves).

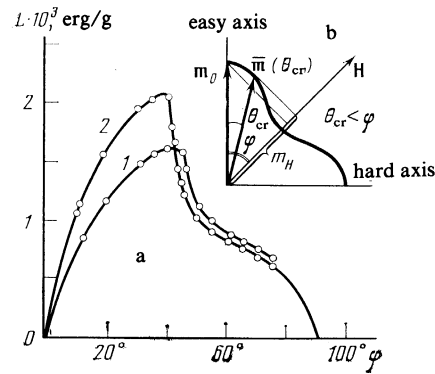


FIG. 6. a: Angular dependence of the torque in $Y_{0.1}Lu_{0.9}CrO_3$ for fields $H = 8$ kOe (1) and $H = 15$ kOe (2) at $T = 4.2$ K. b: Polar diagram showing how the magnetic moment m (proportional to the vector F) moves in an external field as the orientation varies.

the disordering of the vectors $F(\mathbf{r})$ in the angular phase. Indeed, the dependence $\theta(\varphi)$ cannot be smooth for strong fields, because the Zeeman energy of the system will increase if F is rotated by an angle exceeding the critical value (cf. Fig. 6b), so that such rotations are disallowed. Because of the forbidden range of angles at the center of the spin-flip transition, we thus expect to observe jumps in $L(\varphi)$.

Measurements of the angular dependences of the magnetostriction λ_a along the a -axis (Fig. 5b) also confirm that $\theta(\varphi)$ is nonmonotonic for $H = \text{const}$. We see that λ_a (i.e., the deflection of the vector G) becomes appreciable only for $\varphi \sim 45^\circ$ and rapidly approaches the value $\lambda_a \sin^2 \varphi$ when $G \perp H$.

DISCUSSION

We will determine the experimental observables $\langle G \rangle$ and $\langle F \rangle$ by analyzing the thermodynamic potential of the inhomogeneous system, which is of the form

$$\Phi = \lim \frac{1}{V} \int \left\{ \frac{\alpha}{2} (\nabla G)^2 - \frac{\beta(\mathbf{r})}{2} (Gn)^2 - FH \right\} d\mathbf{r},$$

where the first, second, and third terms correspond respectively to the inhomogeneous exchange energy, the competing anisotropy, and the interaction with the external magnetic field. If we average the orientation fluctuations by the method discussed in Ref. 3, we get

$$\begin{aligned} \Phi_{\text{eff}} &= -\frac{K_1}{2} \cos^2 \bar{\theta} + \frac{K_2}{2} \cos^4 \bar{\theta} - F(\bar{\theta})H \cos(\bar{\theta} - \varphi) \\ &= \Phi_{\text{an}}(\bar{\theta}) + \Phi_H(\bar{\theta}) \end{aligned} \quad (2)$$

for the effective thermodynamic potential.

Here $\bar{\theta}$ specifies the orientation of the average ferromagnetic vector, φ is the orientation of the external magnetic field, and the effective anisotropy constants K_1, K_2 in general depend on the angular dispersion $\theta(\mathbf{r})$. They can be expressed approximately in the form

$$K_1 = \bar{\beta}, \quad K_2 = D(\beta)R^2/\alpha + O(D^2(\bar{\theta})),$$

where $\bar{\beta}$ is the average anisotropy constant, $D(\beta)$ is the dis-

person, and R_c is the correlation radius of the anisotropy fluctuations; α is the inhomogeneous exchange parameter. The magnitude of the weak ferromagnetic moment then also depends on its orientation:

$$F(\bar{\theta}) = F_0 \exp \left[-\frac{D(\bar{\theta})}{2} \right] \left\{ 1 - \frac{D(\bar{\theta})}{2} \right\}. \quad (3)$$

The dispersion of the orientation fluctuations is given by the expression

$$D(\bar{\theta}) = d(H, \bar{\theta}) \sin^2 \bar{\theta} \cos^2 \bar{\theta}.$$

For the fields of interest (much weaker than the exchange field), we have

$$d(H, \bar{\theta}) = \left[\frac{H_d}{H_K \cos 2\bar{\theta} + H \cos(\bar{\theta} - \varphi)} \right]^{1/2},$$

where $H_K = H_{K_1} = \beta/F_0$, $H_d = D^2(\beta)R_c^6/F_0\alpha^3$.

The dependence of the magnitude of the average antiferromagnetic vector on the orientation F/F is also described by an equation of the form (3).

We can calculate the equilibrium angles $\bar{\theta}$ from expression (2) for Φ_{eff} . Figure 7 plots the calculated $\bar{\theta}(\varphi)$ dependence for fields $H \gg H_{K_1} > H_{K_2} = K_2/F_0$ for several values of the parameter $d(H) = (H_d/H)^{1/2}$.

The jumps in the dependence $\bar{\theta}(\varphi)$ are striking for H oriented near the diagonal of the ac -plane ($\varphi = 45^\circ$) and can be traced clearly in the curves $\lambda_a(\varphi)$ (Fig. 5b) and in $L(\varphi)$ for the torque (Fig. 6).

We have already noted that these jumps can be ascribed to the dependence (3) of $F(\theta)$; they should therefore occur in general for systems with competing anisotropy.

We now consider the anomalies in the torque curves. Using Eq. (2) derived above for Φ_{eff} , we get the expression for the average torque. We note that the last term is positive for $\bar{\theta} < \pi/4$ and negative for $\bar{\theta} > \pi/4$ since (as pointed out above) $F(\theta)$ has a maximum at $\bar{\theta} = \pi/4$.

The observed anomalies in the torque curves are caused by the oscillatory term in the expression for \bar{L} , in addition to the jumps in $\bar{\theta}(\varphi)$. Figure 8 shows some $L(\varphi)$ curves calculated

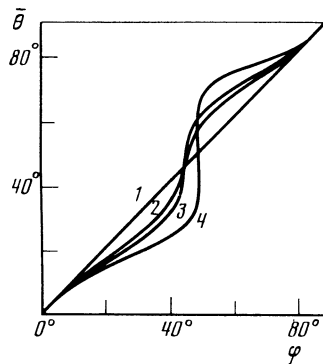


FIG. 7. Dependence $\bar{\theta}(\varphi)$ calculated for fields $H \gg H_K$, H_K , for several values of $d = (H_d/H)^{1/2}$: $d = 0$ (1), 2 (2), 3.5 (3), 5 (4).

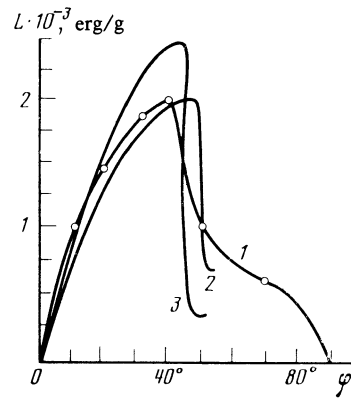


FIG. 8. Angular dependences of the torque in $Y_{0.1}Lu_{0.9}CrO_3$. Curve 1 gives the experimental results for $H = 15$ kOe; curves 2, 3 are calculated for $H = 7$ and 15 kOe, respectively assuming a value ≈ 180 kOe for H_d .

theoretically. Curves 2 and 3, which correspond to different magnetic fields, both exhibit the characteristic drop in $L(\varphi)$ for field orientations $\varphi \approx 45^\circ$ in the ac -plane. Their relative position is in qualitative agreement with the experimental observations (curve 1). Rather good quantitative agreement with experiment is achieved if we take $H_d \approx 180$ kOe, $H_{K_1} = 5.6$ kOe, $H_{K_2} = 2.7$ kOe.

Because this value of H_d is so large, we must assume that the substantial deformations of the $Cr^{3+}-6O^{2-}$ octahedra caused by the different radii of the Y and Lu ions may make the local magnetic anisotropy constant substantially larger than the average magnetic anisotropy energy $\bar{\beta} = 5 \cdot 10^4$ erg/cm of the system (these local constants determine the dispersion $D(\beta)$, which is estimated to be $\lesssim 3 \cdot 10^5$ erg/cm). The values found above for H_d , H_{K_1} , and H_{K_2} enable us to estimate the monoclinic distortions $\lambda_{ac}^{\text{max}}$ for different angles φ . If we recall that (3) implies that $G(\bar{\theta})$ depends on the magnetic field orientation and use the above values for H_d , H_K , we find that

$$\lambda_{ac}^{\text{max}}(\varphi=45^\circ)/\lambda_{ac}^{\text{max}}(\varphi=90^\circ) \approx 4.8,$$

in good agreement with experiment. The large drop in $\lambda_{ac}^{\text{max}}$ for $\varphi = 90^\circ$ is due to the large dispersion of the local orientations $G(r)$ that results when the average antiferromagnetic vector passes through the angle $\bar{\theta} = 45^\circ$. In particular (as in other disordered materials⁸), the vectors $\mathbf{G}(\mathbf{r})$ can make an obtuse angle with the average vector $\langle \mathbf{G} \rangle$.

CONCLUSIONS

Our experimental studies of the torque and magnetstriction curves for $Y_{0.1}Lu_{0.9}CrO_3$ indicate that when a field-induced spin-flip transition occurs from the Γ_2 phase at $T = 4.2$ K, a magnetic structure forms whose average magnetic moment $F(\theta)$ and orientation fluctuation dispersion $D(\theta) = \langle \delta\theta^2 \rangle$ are orientation-dependent. This behavior is typical for systems with competing magnetic anisotropy and is responsible for the characteristic anomalies in the magne-

tostriction and torque curves. We may thus recommend the use of the above methods in experiments on disordered structures.

¹C. M. Hurd, *Usp. Fiz. Nauk* **142**, 331 (1984) [*Contemp. Phys.* **23**, 469 (1982)].

²A. M. Kadomtseva, A. P. Agafonov, et al., *Zh. Eksp. Teor. Fiz.* **81**, 700 (1981) [*Sov. Phys. JETP* **54**, 374 (1981)].

³E. V. Sinityn and I. G. Bostrem, *Zh. Eksp. Teor. Fiz.* **85**, 661 (1983) [*Sov. Phys. JETP* **58**, 385 (1983)].

⁴A. M. Kadomtseva, G. G. Artem'ev, et al., *Pis'ma Zh. Eksp. Teor. Fiz.* **38**, 383 (1983) [*JETP Lett.* **38**, 463 (1983)].

⁵A. S. Moskvina and E. V. Sinityn, *Kristallografiya*. **22**, 376 (1976) [*sic*].

⁶A. M. Kadomtseva, A. P. Agafonov, et al., *Fiz. Tverd. Tela (Leningrad)* **23**, 3554 (1981) [*Sov. Phys. Solid State* **23**, 2065 (1981)].

⁷K. N. Belov, A. K. Zvezdin, A. M. Kadomtseva, and R. Z. Levitin, *Spin Flip Transitions in Rare-Earth Magnets* [in Russian], Nauka, Moscow (1979).

⁸V. L. Ginzburg, *Zh. Eksp. Teor. Fiz.* **77**, 236 (1979) [*Sov. Phys. JETP* **50**, 120 (1979)].

Translated by A. Mason